Saudi Journal of Biological Sciences 28 (2021) 484–491

Contents lists available at ScienceDirect

Saudi Journal of Biological Sciences

journal homepage: www.sciencedirect.com

Original article

Carbon nanotubes catalyzed UV-trigger production of hyaluronic acid from *Streptococcus equi*

Yasser A. Attia [a,*], Ashwaq M. Al Nazawi [b], Hassan Elsayed [c], Mahmoud W. Sadik [d]

[a] National Institute of Laser Enhanced Sciences, Cairo University, Giza 12613, Egypt
[b] Preventive Medicine Department, Public Health Directorate, Ministry of Health, Jeddah 22246, Saudi Arabia
[c] Department of Microbial Biotechnology, Genetic Engineering and Biotechnology Division, National Research Centre, Dokki, Giza 12622, Egypt
[d] Microbiology Department, Faculty of Agriculture, Cairo University, Giza 12613, Egypt

ARTICLE INFO

Article history:
Received 6 September 2020
Revised 5 October 2020
Accepted 19 October 2020
Available online 28 October 2020

Keywords:
Hyaluronic acid
Streptococcus Equi
UV-photoproduction
Carbon nanotubes
Catalysts

ABSTRACT

Hyaluronic acid (HA) has great importance in biomedical applications. In this work, a novel nanoparticle-based method that stimulates the hyaluronic acid (HA) production by the bacteria *Streptococcus equi* subsp. Zooepidemicus has been reported. CNTs with diameters of 40–50 nm and lengths of about 20 mm were used at four different concentrations (0, 10, 25, 50, and 100 μg) to the bacteria and determined the mass of the produced HA in dependence on the exposure time under UV-irradiation. The results clearly showed that the exposure for one minute with low power UV light (254 nm) and 100 μg (CNTs) treatments steadily increased HA production from the control (0.062 g/L) to the highest value (0.992) g/L of HA. The incubation of the streptococci with CNTs led to an increase of the HA production by a factor of 4.23 after 300S exposure time under UV light, whereas the HA production was no significant enhancement under visible light. It is explained that the CNTs nanoparticle-stimulated increase of the HA production with the internalization of the nanoparticles by the bacteria since they "serve as co-enzymes" under induced mutation by UV-irradiation. Transformation process was carried out and showed that the major protein band of *Streptococcus equi* was observed in the Streptococcus DH5α. RAPD analysis indicates that the amplified DNA fragments and the percentage of polymorphism was similar between *Streptococcus equi* and Streptococcus DH50α. The chemical structure and molecular weight of the photoproduced HA from *Streptococcus equi* was similar to the chemical structure of the standard sample.

1. Introduction

Hyaluronan (HA) was first discovered and isolated in 1934 from the vitreous humor of bovine as an acid by Karl Meyer and John Palmer. HA is a nonsulfated glycosaminoglycan (GAG) component of the extracellular matrix [Lepidi et al. 2006]. It occurs naturally in vertebrate tissue and body fluids. It is found in relatively high concentrations in the vitreous humor of the eye, umbilical cord, synovial joint fluid, and rooster combs. HA is a large and unbranched molecule and has a repeating disaccharide structure of N-acetylglucosamine and glucuronic acid [Prawel et al. 2014]. As a polysaccharide, HA has a unique combination of properties. HA is viscoelastic, where HA solutions are primarily viscous at a low shear rate and elastic at a high shear rate. This is thought to be associated with the single carboxyl group (–COOH) per disaccharide unit of HA. The carboxyl group dissociates at a physiological pH, producing polyanionic properties. The negatively charged chains can expand and entangle at low concentrations, which can contribute to viscoelastic properties [Gong et al. 2010]. The viscoelastic properties of HA make it an effective lubricant. HA is present in the intima and adventitia of all blood vessels, and it can be found in the media with the less homogeneous distribution. The amount of HA present in blood vessels depends on the age and type of vessel, ranging from 40% to 4% of the total glycosaminoglycan content in the fetal umbilical artery compared to the adult aorta, respectively. The higher HA content in younger vessels results in a loose, hydrated, and flexible extracellular matrix. Multiple studies have reported that HA plays a role in endothelial cell

* Corresponding author.
E-mail address: yasserniles@niles.edu.eg (Y.A. Attia).

Peer review under responsibility of King Saud University.

Production and hosting by Elsevier

https://doi.org/10.1016/j.sjbs.2020.10.032
1319-562X/

proliferation, migration, and retention [Prawel et al. 2014]. It has also been shown that HA functions in the formation of new blood vessels. HA is non-toxic, biodegradable, biocompatible, nonimmunogenic, and has receptor-binding properties. HA and its derivatives have been investigated extensively for biomedical applications, such as tissue engineering, arthritis treatment, ocular surgery, drug delivery, and molecular imaging [Jiang et al. 2011; Duncan, 2003; Torchilin, 2007; Zhu et al. 2016; Oh et al. 2010].

HA has also been used in nanoparticles for drug delivery [Gaffney et al. 2010], synovial fluid in arthritic patients, cosmetic surgery, cosmetic and soft tissue surgery, and abdominal procedures. It is also used as a diagnostic marker for cancer, rheumatoid arthritis, liver disease, and organ transplantation rejection [Volpi et al. 2009]. Medical devices, including catheters, guidewires, and sensors use HA to increase lubricity and decrease biofouling. Additional applications of HA include viscosupplementation, viscoseparation, viscosurgery, viscoaugmentation, drug delivery, wound repair, medical devices, and other applications of tissue engineering [Prawel et al. 2014]. Previous studies indicate that these qualities of HA depend on the molecular weight of the HA monomers. High molecular weight HA (1500 kDa) is naturally anti-inflammatory and immunosuppressive, thereby inhibiting the migration of free-radical producing microbes into other tissues. On the other hand, low molecular weight HA (0.75–10 kDa) interacts with cell receptors to induce multiple signaling cascades [Ibrahim and Ramamurthi, 2008].

Although HA can be extracted from animal tissues or bacterial fermentation, infectious agents can cause contamination of animal-derived products, and that has made the bacterial fermentation a more desirable production system. However, HA from bacterial sources is of a lower molecular weight compared with that extracted from animal tissues. Previously reported studies presented development to the production of HA from bacterial fermentation of Streptococcus *Equi* or *zooepidemicus* with high molecular weight of HA polymers [Attia et al. 2018; Chong and Nielsen, 2003; Hu et al. 2004]. Recently, nanomaterials as additives can be a promising technique to address the needs of HA production [Attia et al. 2018; Choi et al. 2009; Saravanakumar et al. 2010; Park et al. 2015; Vázquez et al. 2015]. The HA has great value (200 mg HA made are sold at a rate of 800 US Dollars). Therefore, innovative production methods and novel HA biomaterials for tissue engineering and improved properties of viscosupplements are desired.

Herein, the present work aims to improve the HA production by the microorganism, *Streptococcus Equi,* using CNTs under UV-irradiation as a substitute to that found in the animal and plant sources, which are very expensive and produced in small quantities. In addition, one of the objectives of this work is to identify a bacterial hyaluronic acid, and its production, purification, and fractionation.

2. Materials and methods

2.1. Microbiological culture media and growth conditions of bacterial strains

Streptococcus Equi subsp. *zooepidemicus* (ATCC® 35246™), bacteria-strains purchased from the American Type Culture Collection (Manassas, VA, USA) were used in the HA production. The bacterium stocks were stored in complex medium with 25% glycerol at −80 °C. The complex and alternative growth media for *Streptococcus Equi* subsp. *zooepidemicus* contained the following nutrients: 50 g/L of glucose, 5 g/L of yeast extract, 2 g/L of K_2HPO_4, 2 g/L of KH_2PO_4, 0.5 g/L of $MgSO_4$, 0.5 g/L of $(NH_4)SO_4$, and 15 g/L tryptone (Cultimed, PanreacQuímica, Spain). After autoclaving and sterilized at 121 °C/15 min, the pH was adjusted to 7 in all cultures. In a glass 2 L bioreactor, the stains were cultivated at 37 °C, 500 rpm of agitation, without aeration, and pH-controlled with sterile solutions of NaOH and HCl. Glucose was added every 2 h (from 8 to 10 h of culture) up to 20 g/L using a sterile glucose solution of 500 g/L in the fed-batch cultivations [Attia et al. 2018; Vázquez et al. 2015].

2.2. Effect of ultra-violet (UV) irradiation on hyaluronic acid production

Low power ultraviolet lamp (254 nm) was fixed at 25 cm in a tightly closed wooden chamber [Gardner et al. 1991]. An aliquot of *Streptococcus Equi* cells grown in the complex medium for 16–18 h was exposed to the low power UV-irradiation (254 nm). During the exposure time, it was gently agitated on a vibratory shaker. The mutants were isolated at different times (zero – 5 min.). The mutant cells were plated into complex and minimal medium agar plates after the cultures were diluted serially into sterile 0.85% NaCl and incubated for 24 h at 37 °C. The same experiment was repeated but under visible light irradiation.

2.3. Effect of carbon nanotubes (CNTs) on hyaluronic acid production

After exposed vegetative cells of *Streptococcus Equi* to visible light and UV irradiation for 0–5 min and wild type were grown in tryptone soybean broth (TSB) for 16 h at 37 °C. During the irradiation, different amounts (0, 10, 25, 50, and 100 μg) of CNTs were added to 2 mL of cell suspension and then incubated for 60 min. in a shaking incubator. Then, centrifuged for 5 min at 3000 rpm. Then, the treated cells were suspended in 2 mL sodium phosphate buffer, (50 mM) at pH 6.2. This suspension was diluted serially and the appropriate dilutions were plated onto M17 agar [Kamal et al. 2001].

2.4. Transformation

2.4.1. A purification of plasmid DNA by PEG precipitation

To the plasmid containing supernatant, an equal volume of 1.6 mM NaCl and 13% (w/v) polyethylene glycol (PEG 8000) was added and the mixture was incubated on ice for 1 h. The DNA was recovered by centrifugation for 15 min. at 14,000 rpm. The pellet was washed thrice with cold 70% ethanol and resuspended in TE buffer (pH8.0).

2.4.2. Medium scale isolation and purification of plasmid by Qiagen column (Qiagen GmbH)

25 mL (high copy number) or 100 mL (low copy number), overnight grown culture of bacterial cells, was harvested by centrifugation at 5000*g* at 4 °C. The pellet was dissolved in 4 mL or 10 mL solution I (25 mM Tris-HCl, pH 8.0, 10 mM EDTA, 50 mM glucose). These cells were lysed by adding 4 mL or 10 mL of solution II (0.2 N NaOH, 1% SDS freshly prepared); this was gently mixed by inversion and kept at room temperature for 5 min. Following this, chilled (ice cold) 4 or 10 mL of solution III (3 M potassium acetate pH 4.8, glacial acetic acid 11.5 mL, 1 mL H_2O) was added and mixed by inversion. This mixture was incubated on ice for 20 min. and supernatant was collected after centrifugation at 12,000 rpm at 4 °C for 30 min. The supernatant was then loaded onto the Qiagentip-100, pre-equilibrated with solution QBT (700 mM NaCl, 50 mM MOPs pH 7.0, 15% isopropanol, and 0.15% Triton × 100) and allowed to pass under gravity. The Qiagen tip was washed twice with 10 mL or 30 mL of buffer QC (1.0 M NaCl, 50 mM MOPs, pH 7.0, and 15% isopropanol solution). Then, the plasmid DNA was eluted by 5 or 15 mL of solution QF (1.25 M, NaCl, 50 mM MOPs, pH 7.0, and 15%, isopropanol). This was finally precipitated by

0.7 vol of isopropanol at room temperature and after centrifugation, the plasmid pellet was collected. Finally, the plasmid DNA was washed with 70% ethanol, vacuum dried and dissolved twice in minimal volume of TE (Tris-EDTA buffer, pH 8.0).

2.4.3. Preparation of competent cells and transformation

αDH5á competent cells were prepared [Hanahan, 1985]. A single colony of DH5a was picked up and inoculated into 5 mL LB medium (Luria-Broth) and grown overnight at 37 °C. One mL of this was inoculated freshly into 100 mL of LB (luria-broth medium) and grown at 37 °C for 3 h, till the O.D (optical density) of 0.5–0.6 was obtained. The cells were harvested by centrifugation at 3000 rpm for 10 min. The pellet was resuspended in 40 mL of Tfb1 solution (3 mM CH_3 COOK, 5 mM $MgCl_2$, and 100 mM $CaCl_2$) at 4 °C, centrifuged and the pellet was resuspended in 4 mL of Tfb2 solution (10 mM Na-MOPs, pH 7.0, 75 mM $CaCl_2$, 10 mM KCl and 15% glycerol). The cell suspension (0.1 mL) was aliquoted into Eppendorf tubes, frozen immediately in liquid nitrogen and stored at −80 °C.

This was subjected to heat shock by incubating at 42 °C for 90 sec. and then immediately transferred to 4 °C for 10–20 min followed by addition of 900 μl of LB and then grown at 37 °C with slow shaking. Different aliquots of these transformed competent cells were plated on to LB plate containing 100 μg/mL of flummox or 100 μg/mL cefuroxiime oxetil.

2.4.4. Polymerase chain reaction

Taq-polymerase, dNTPs (deoxynucleotide triphosphate) and convergent primers achieved amplification of the DNA fragment.

Table 1
Sequences of K1 and K2 primers.

Type of primer	The sequence
K1	5⁻-TGCCGAGCTG-3⁻
K2	5⁻-GTGAGGCGTC-3⁻

The reaction conditions for PCR involved denaturation at 94 °C for 30 s, annealing at 52 °C for 30 s and extension at 72 °C for either 30 s for cloned DNA in plasmid or 2.5 min (for 2AII promoter amplification) and 2 min (for CA PRO + GUS fusion). After 30 cycle of amplification, an aliquot of this reaction mixture was loaded onto a 0.8% agarose gel and checked (table 1).

2.4.5. SDS-PAGEs

SDS-PAGE was performed [Laemmli, 1970].

2.4.6. Protein estimation

Estimation of protein concentrations in various extracts was determined [Bradford, 1976].

The statistical analysis was performed by GraphPad Prism software (version 7, CA, USA) using paired *t* test. Quantitative summary data are shown as means ± standard errors of the means (SEM) as indicated in the figure legends of the resulting analysis.

3. Results

Carbon nanotubes (CNTs) were purchased from the scientific excellence center, ministry of military Production, Egypt. CNTs with diameters of 40–50 nm and lengths of about 20 mm are shown in Fig. 1a. The chemical composition of CNTs was analyzed by an energy dispersive spectrometer (EDS) spectrum via SEM (Fig. 1b). The results show the presence of (C and O) with (91.08 wt% and 7.92 wt%) confirming the sample is of high purity. In Fig. 1c, it was shown that the XRD pattern of CNTs contained characteristic diffraction peaks at t 26.52°, 42.48°, 54.71°, and 77.43° 2θ, owing to (220), (100), (004), and (110) reflection of planes, respectively. The CNTs showed surface area (N_2 BET) of 57 m^2 g^{-1}. In Fig. 1d, the FTIR spectrum of the purchased CNTs showed a broad absorption peak corresponding to –OH group in the range of 3450–3460 cm^{-1}. The C-H stretch vibration peaks

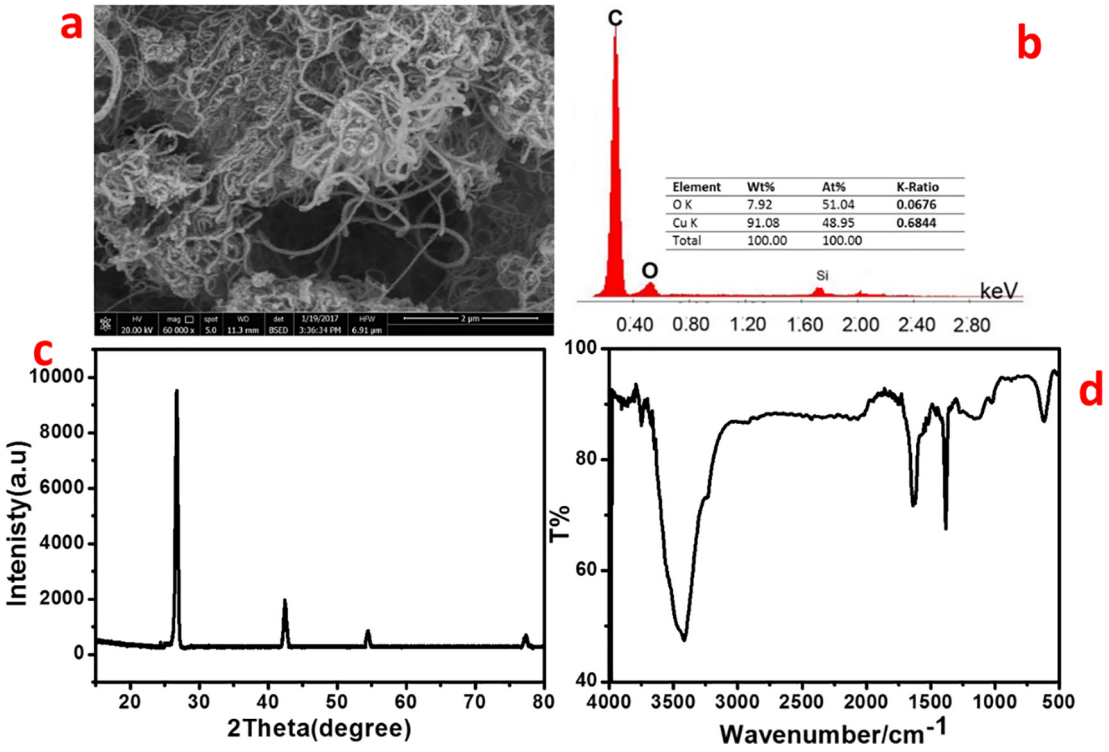

Fig. 1. SEM image of the produced CNTs (a), EDS spectrum (b), XRD pattern (c) and FTIR spectrum (d).

were observed at 2950 and 2850 cm^{-1}. The peak at 1580 cm^{-1} corresponds to C-C vibration. Another peak at 1650 cm^{-1} is the C-O stretching mode of the functional groups on the surface of the MWCNTs. The peak appeared at 950 cm^{-1} corresponds to the C-O stretching mode [He et al. 2011; Altalhi et al. 2016].

Table 2
Effect of UV–Visible irradiation on hyaluronic acid production by *streptococcus Equi*. Each value represents the mean ± SE.

UV – exposuretime (Seconds)	Dry weight of hyaluronic acid (g/l)	Visible – exposuretime (Seconds)	Dry weight of hyaluronic acid (g/l)
0.0	0.062 ± 0.00325	0.0	0.062 ± 0.00325
30	0.065 ± 0.00727	30	0.063 ± 0.00176
60	0.099 ± 0.00465	60	0.065 ± 0.00251
90	0.109 ± 0.00491	90	0.066 ± 0.00769
120	0.118 ± 0.00618	120	0.066 ± 0.00128
150	0.123 ± 0.00580	150	0.067 ± 0.00441
180	0.131 ± 0.00309	180	0.068 ± 0.00235
210	0.139 ± 0.00562	210	0.068 ± 0.00854
240	0.143 ± 0.00368	240	0.069 ± 0.00012
270	0.133 ± 0.00719	270	0.07 ± 0.00633
300	0.126 ± 0.00309	300	0.07 ± 0.00528

3.1. Effect of Ultra-violet (UV) irradiation on hyaluronic acid production

HA was precipitated, recovered and dried from the broth as described [Attia et al. 2018]. Bacterial cell suspension of *Streptococcus Equi* cells were exposed to low power UV light (254 nm) and to visible light (HALOPAR halogen lamp, 75 W). The statistical analysis of the various groups of treated samples shows that all the employed treatments have resulted in different HA production. Such differences are statistically highly significant ($p < 0.001$) for UV group versus visible light irradiation group.

Data in the Table 2 shows clearly that after 4 min of exposure to UV-irradiation, HA production increased to 0.143 ± 0.003 g/L compared to 0.062 ± 0.00325 g/L at 0 min. At longer UV exposure time, HA production was decreased to 0.133 ± 0.007 g/L and 0.126 ± 0.003 g/L at 4.5 and 5 min, respectively. However, after 5 min under visible light irradiation, there was a slight increase in HA production from 0.062 ± 0.00325 g/L at 0 min to 0.07 ± 0.00325 g/L at 5 min as shown in Fig. 2.

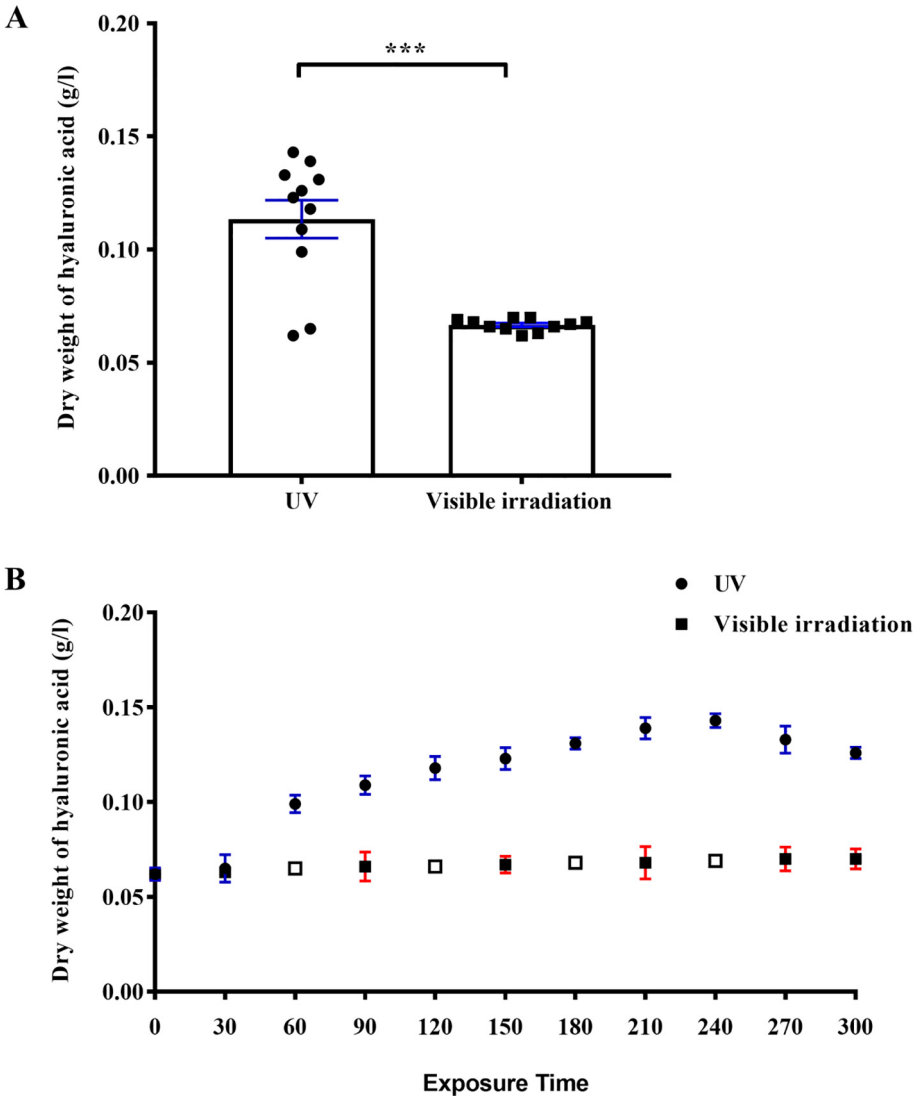

Fig. 2. The impact of UV/Visible irradiation on hyaluronic acid production by *streptococcus Equi*. The hyaluronic acid production at all-time point (A). Hyaluronic acid production at specific exposure time (B). Each value represents the mean ± SEM. Statistical significance of differences was determined by Paired *t* test, ***$p < 0.001$ UV group versus visible light irradiation group. The empty bars represent the error bars that are shorter than the height of the symbol.

3.2. Effect of carbon nanotubes (CNTs) on hyaluronic acid production

Streptococcus Equi cells that gave the highest hyaluronic acid production after mutagenesis by UV treatment were subjected to CNTs. Table 3 shows the effect of (CNTs) on hyaluronic acid production by *Streptococcus Equi* under visible light irradiation. Vegetative cells were exposed to different amounts of CNTs (0, 10, 25, 50, and 100 μg) for different periods (0–300 s) as shown in Table 3 and after exposure to UV irradiation as shown in Table 4 and Fig. 3. The impact of UV/Visible irradiation exposure time on hyaluronic acid heatmap production by *streptococcus Equi* is shown Fig. 4. Results clearly show that hyaluronic acid production was decreased by increasing CNTs concentration under visible light irradiation. The highest hyaluronic acid production was obtained after 240 and 180 s with 50 and 100 μg of CNTs, respectively under visible light irradiation. The highest concentration may be toxic to the cells. It was clearly shown the size-dependent toxicity of carbon nanotubes on microbial cells. Attachment of such carbon nanomaterials on cell clumps led to hypersensitive responses and cell death occurs either by apoptosis or necrosis [Tan et al. 2009]. However, the mutagenic treatment with UV-light proved to be effective over CNTs for the enhancement of hyaluronic acid production by *Streptococcus equi.* The highest hyaluronic acid production was obtained 0.627 g/L and 0.992 g/L after 300 s with 50 and 100 μg of CNTs, respectively under UV light irradiation (Fig. 3). Generally, the addition of CNTs has been shown to significantly produce more HA from treated samples under UV irradiation.

3.3. Studies of the chemical structure of hyaluronic acid

The polysaccharide produced from *Streptococcus Equi* was isolated by ethanol precipitation of the protein-free culture supernatant. The bacterial mucopolysaccharide precipitate was subjected to chemical analysis, the results of which are summarized in Table 5. The chemical analysis of HA shows that the sample contains glucuronic acid, N-acetyl glucosamine, and nitrogen (47.99%, 36.57%, and 4.7%), respectively. The sample also showed moisture by 10.74% with no protein and ash detected by the buriet method.

It is clear from the Table 5 that the purified exopolysaccharide was contained glucuronic acid and N-acetyl glucosamine with a molar ratio 1.041. Meyer and Plamer pointed out that the polysaccharides had high molecular weights from the vitreous humor of cattle eyes and umbilical cord [Meyer and Palmer, 1943]. It was composed of an equal number of N-acetylglucosamine (20.5%) and glucuronic acid residues (20.5%). The calculated molecular weight of the purified sample HA was 1.48×10^6 da compared to the standard sample of HA 1.45×10^6 da and these results are in agreement with those reported [Kakizaki et al.2002].

3.4. Transformation

In attempt to increase the number of mutant cells from *Streptococcus equi* and decrease the time of production of hyaluronic acid plasmid was transformed to *E. coli* (αDH5ā) and to show expression of (A) *Streptococcus equi* and (B) *Streptococcus* $DH_{5\alpha}$. SDS-PAGE was performed and expressions of (A) and (B) were seen on gel (Fig. 5). Cells with *Streptococcus equi* served as control for *E. coli.*

Expression of the *Streptococcus equi* protein was tested in *E. coli* for the induction of *Streptococcus equi* protein, in which the *Streptococcus equi* plasmid was transformed into *E. Coli* cells. The *E. coli* cells were grown to 0.4 O.D as a control, *Streptococcus equi* cells containing the same plasmid were also grown. It can be seen from

Table 3
Hyaluronic acid production after treatments of *streptococcus Equi* (wild type) with carbon nanotubes (CNTs) with different concentrations for different times under visible light irradiation. Each value represents the mean ± SE.

Time (Sec.)	Dry weight of hyaluronic: acid g/L			
	Concentrations of CNTs (μg)			
	10	25	50	100
0.0 (Wild type)	0.062 ± 0.003	0.062 ± 0.003	0.062 ± 0.003	0.062 ± 0.003
30.0	0.063 ± 0.002	0.069 ± 0.0012	0.078 ± 0.011	0.086 ± 0.001
60.0	0.076 ± 0.011	0.09 ± 0.022	0.102 ± 0.002	0.112 ± 0.003
90.0	0.083 ± 0.005	0.117 ± 0.043	0.128 ± 0.003	0.141 ± 0.001
120.0	0.091 ± 0.023	0.133 0.017	0.155 ± 0.001	0.169 ± 0.003
150.0	0.102 ± 0.032	0.158 ± 0.082	0.181 ± 0.002	0.198 ± 0.002
180.0	0.112 ± 0.071	0.197 ± 0.062	0.212 ± 0.002	0.274 ± 0.001
240.0	0.126 ± 0.034	0.221 ± 0.013	0.242 ± 0.007	0.257 ± 0.003
300.0	0.139 ± 0.002	0.232 ± 0.081	0.239 ± 0.002	0.244 ± 0.001

Table 4
Hyaluronic acid production after treatments of *streptococcus Equi* (wild type) with carbon nanotubes (CNTs) with different concentrations for different times under UV-light irradiation. Each value represents the mean ± SE.

Time of UV-exposure (Sec.)	Dry weight of hyaluronic: acid g/L			
	Concentrations of CNTs (μg)			
	10	25	50	100
0.0 (Wild type)	0.062 ± 0.003	0.062 ± 0.003	0.062 ± 0.003	0.062 ± 0.003
30.0	0.066 ± 0.005	0.099 ± 0.0005	0.112 ± 0.014	0.140 ± 0.029
60.0	0.110 ± 0.036	0.123 ± 0. 036	0.185 ± 0.037	0.207 ± 0.004
90.0	0.12 ± 0.0035	0.157 ± 0.014	0.263 ± 0.002	0.348 ± 0.005
120.0	0.127 ± 0.021	0.196 0.004	0.322 ± 0.003	0.502 ± 0.001
150.0	0.149 ± 0.065	0.242 ± 0.065	0.407 ± 0.091	0.638 ± 0.082
180.0	0.172 ± 0.032	0.295 ± 0.013	0.497 ± 0.021	0.752 ± 0.064
240.0	0.188 ± 0.089	0.327 ± 0.028	0.589 ± 0.097	0.877 ± 0.019
300.0	0.234 ± 0.013	0.377 ± 0.021	0.629 ± 0.032	0.992 ± 0.002

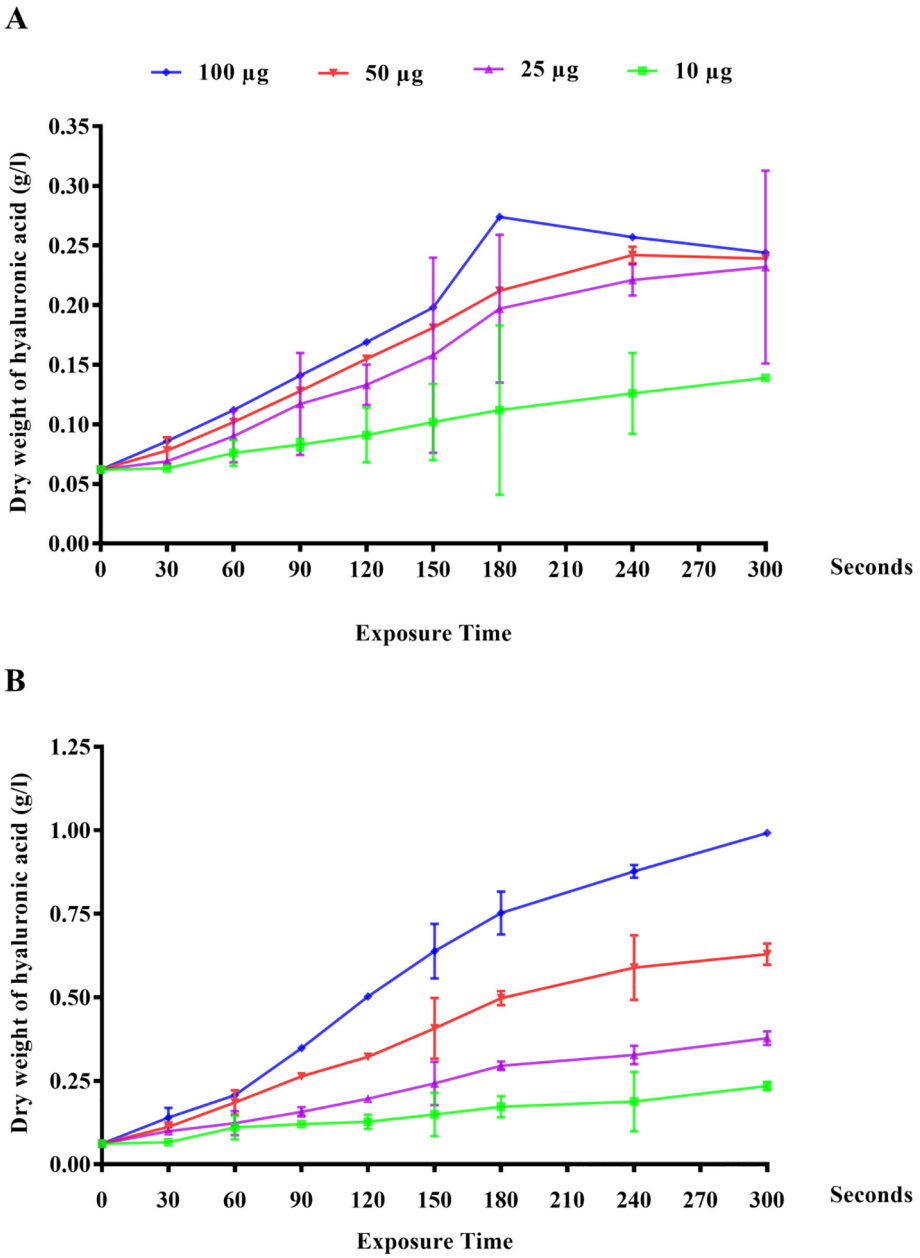

Fig. 3. Hyaluronic acid production after treatments of *streptococcus Equi* (wild type) with carbon nanotubes (CNTs) with different concentrations for different times under visible light irradiation (A), UV-light irradiation (B) Each value represents the mean ± SEM.

Fig. 6 that a major protein band of *Streptococcus equi* was observed in the *Streptococcus* $DH_{5\alpha}$ cultures. The size of the protein corresponded to the expected size for *Streptococcus equi* protein.

One of the most objectives of the present study was to determine genetic similarity between *Strepto-equi* and *Strepto-DH5α* after transformation by *Strepto-equi* plasmid based on RAPD markers and identify the relation between two strains. RAPD analysis was performed using two random primers. The selected random primers were RAPD1 and RAPD2. Data presented in Table 1 show the sequence of the selected random primers. Only visible and reproducible major bands were considered, while minor, irreproducible and smeared bands were canceled. A glance on data presented in Fig. 6 indicates that the amplified DNA fragments and the percentage of polymorphism was similar between *Strepto-equi* and Sstrepto-DH5α. The data tabulated in Table 1 indicated that the primer RAPD1 is the most efficient primer for generating polymorphism with *Strepto-*$DH_{5\alpha}$.

4. Discussion

These changes in HA production due to UV induced mutants that were more stable through the long term of generations and subculturing [Thoma, 1971]. In addition, exposure to UV irradiation stimulates tolerance to different environmental stresses, changes in protein synthesis, and increased activity of biosynthesis enzymes [Hartke et al. 1995]. These results in agreement with that reported by Saranraj et al. (2011) which irradiated *Streptococcus pyrogens* with UV light for 10 min, which was due to UV mutation produces a workable effect on HAS gene (hyaluronate synthase gene) and mutation with UV irradiation improves hyaluronic acid

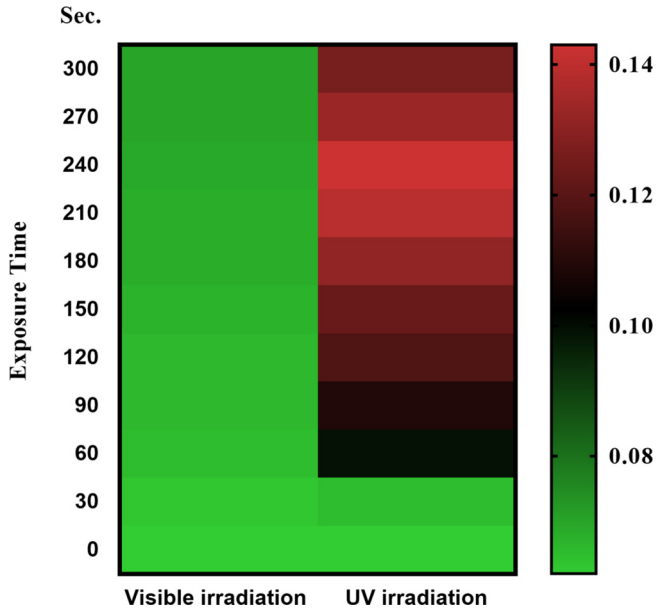

Fig. 4. The impact of UV/Visible irradiation exposure time on hyaluronic acid heatmap production by *streptococcus Equi*.

Table 5
Molar ratio of hyaluronic acid that produced from *Streptococcus equi* after complete hydrolysis with 1 N HCl and determined by HPLC.

Source of hyaluronic acid	Glucouronic acid (mg /10 mg)	N-acety\glucosaraine (mg/l0mg)	Molar ratio
Standard (sigma)	6.001	5.78	1.038
Sample	3.53	3.4	1.041

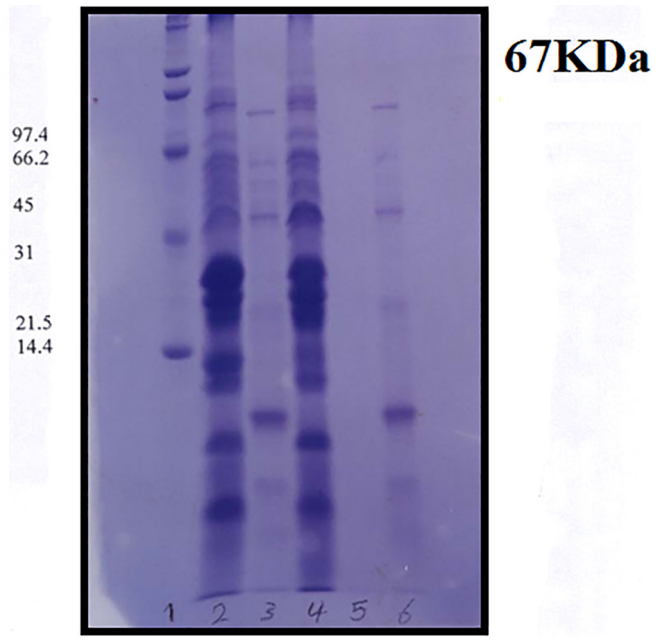

Fig. 5. Proteins expression shown on SDS-PAGE for *Streptococcus equi* after different treatment by (Orginal, CNTS, UV, UV-CNTS, Transformed and *E. coli*). Aliquots of each sample were solubilized in sample buffer and electrophoresed on a 10% SDS-PAGE gel.

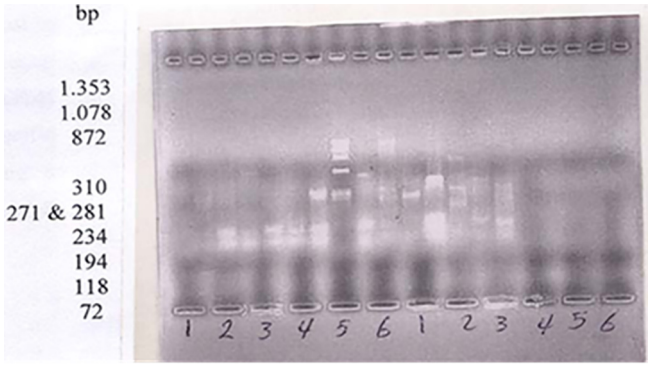

Fig. 6. Agarose gel (1%) electrophoresis of PCR products obtained with universal primers for *Streptococcus equi* (*1-Streptococcus equi* (original strain), *2-Streptococcns equi* after UV irradiation, 3-*Streptococcus equi* after UV + CNTs, *4-Streptococcus equi* - *E. coli* (DH5a), and *5-Kcoli (DH5a)* 6-Primer (Hea III)).

production. Also, exposure of DNA to UV light for long time leads to the formation of various kinds of DNA damage, including the *cis-syn* thymine cyclobutane dimer lesion, hereafter called the thymine dimer which causes frame shift and blocking for protein synthesis. Then the DNA damage causes death to the microbial cells and decreases HA production at long irradiation time [Rumora et al. 2008].

The presence of CNTs that absorbs strongly the UV light, prevents the thymine dimer formation. Thus, DNA damage due to the UV exposure decreases and enhances the production of HA. According to our previous study, the enhancement in the HA production is also attributed to the fact that the nanoparticles which are nutrients for the bacterial cells can be absorbed by the bacterial cells in a much higher uptake rate compared to the micronutrients. These nutrients are needed by the bacterial cells and serve as co-enzymes that biostimulated the cells of *Streptococcus Equi* to produce a higher dry weight of HA compared to the control [Attia et al. 2018; Abdelsalam et al., 2016, 2017a, 2017b, 2019]. The CNTs uptake and HA production mechanism is shown Fig. 7.

5. Conclusion

We successfully designed an efficient approach for enhancement hyaluronic acid (HA) production from *Streptococcus Equi* using carbon nanotubes (CNTs) as additives under UV-light irradiation. CNTs treatments stimulated the bacterial cells to increase the hyaluronic acid production under induced mutation by UV-irradiation. At the same time, transformed *Streptococcus equi* plasmid to *E. Coli* $DH_{5\alpha}$ cells increased the number of mutant cells and decreased the production time of hyaluronic acid. Transformation process show that major protein band of *Streptococcus equi* was observed in the *Streptococcus* $DH_{5\alpha}$. RAPD analysis indicates that the amplified DNA fragments and the percentage of polymorphism was similar between *Streptococcus equi* and *Streptococcus* DH50α. The chemical structure of the photoproduced HA from *Streptococcus Equi* was similar to the chemical structure of the standard sample. The molar ratio of glucuronic acid and N–acetyl glucosamine was 1: 1.041 compared with standard sample (1:1.03). This approach provides a new cost-effective and highly hyaluronic acid production.

6. Authors' contributions

YA and MS conceived and designed research. YA conducted experiments. MS contributed new reagents or analytical tools. YA

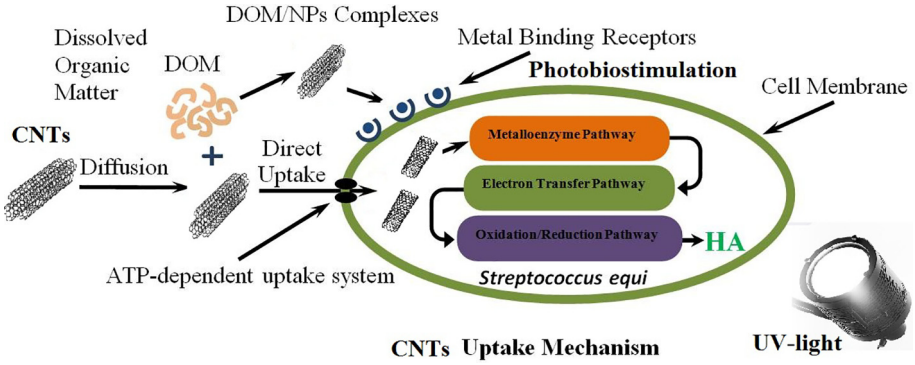

Fig. 7. The CNTs uptake mechanism for HA production by *streptococcus Equi.*

and HE analyzed data. YA wrote the manuscript. All authors read and approved the manuscript.

Funding

This research did not receive any specific grant from funding agencies in the public, commercial, or not-for-profit sectors.

Declaration of Competing Interest

The authors declare no conflicts of interest.

Acknowledgements

We want to acknowledge Mr Mohamed Taha and the members of NILES for their help and support.

References

Abdelsalam, E., Samer, M., Attia, Y., Abdel-Hadi, M.A., Hassan, H.E., Badr, Y., 2017a. Influence of zero valent iron nanoparticles and magnetic iron oxide nanoparticles on biogas and methane production from anaerobic digestion of manure. Energy 120, 842–853.

Abdelsalam, E., Samer, M., Attia, Y., Abdel-Hadi, M.A., Hassan, H.E., Badr, Y., 2017b. Effects of Co and Ni nanoparticles on biogas and methane production from anaerobic digestion of slurry. Energy Convers. Manage. 141, 108–119.

Abdelsalam, E., Samer, M., Attia, Y., Abdel-Hadi, M.A., Hassan, H.E., Badr, Y., 2016. Comparison of nanoparticles effects on biogas and methane production from anaerobic digestion of cattle dung slurry. Renew. Energy 87 (1), 592–598.

Abdelsalam, E., Samer, M., Attia, Y., Abdel-Hadi, M.A., Hassan, H.E., Badr, Y., 2019. Effects of laser irradiation and Ni nanoparticles on biogas production from anaerobic digestion of slurry. Waste Biomass Valorizat. 10, 3251–3262.

Altalhi, T., Mezni, A., Aldalbahi, A., Alrooqi, A., Attia, Y., Santos, A., Losic, D., 2016. Fabrication and characterisation of sulfur and phosphorus (S/P) co-doped carbon nanotubes. Chem. Phys. Lett. 658, 92–96.

Attia, Y.A., Kobeasy, M.I., Samer, M., 2018. Evaluation of magnetic nanoparticles influence on hyaluronic acid production from *Streptococcus equi*. Carbohydr. Polym. 192, 135–142.

Bradford, M.M., 1976. A rapid and sensitive method for the quantification of microgram quantities of protein utilizing the principle of protein-dye binding. Anal. Bioch. 72, 248–254.

Choi, K.Y., Min, K.H., Na, J.H., Choi, K., Kim, K., Park, J.H., Kwon, I.C., Jeong, S.Y., 2009. Self-assembled hyaluronic acid nanoparticles as a potential drug carrier for cancer therapy: synthesis, characterization, and *in vivo* biodistribution. J. Mater. Chem. 19, 4102–4107.

Chong, B.F., Nielsen, L.K., 2003. Amplifying the cellular reduction potential of *Streptococcus zooepidemicus*. J. Biotechnol. 100, 33–41.

Duncan, R., 2003. The dawning era of polymer therapeutics. Nat. Rev. Drug Discovery 2, 347–360.

Gaffney, J., Matou-Nasri, S., Grau-Olivares, M., Slevin, M., 2010. Therapeutic applications of hyaluronan. Moluclar. Biosystems 6, 437–443.

Gardner, E.J., Simmons, M.J., Snustand, D.P., 1991. Mutation. In: Principles of Genetics. 8th ed. Jhon Wiley and Sons Inc New York, pp. 288–319.

Gong, F., Lu, Y., Guo, H., Cheng, S., Gao, Y., 2010. Hyaluronan Immobilized Polyurethane as a Blood Contacting Material. Int. J. Polym. Sci. Article ID 807935.

Hanahan, D., 1985. Heritable formation of pancreatic-cell tumours in transgenic mice expressing recombinant insulin/simian virus 40 on cogenes. Nature 315, 115–122.

Hartke, A., Bouche, S., Laplace, J., Benachour, A., Boutibonnes, P., Auffray, Y., 1995. UV-inducible proteins and UV-induced cross-protection against acid, ethanol, H_2O_2 or heat treatments in *Lactococcus lactis* subsp. *Lactis*. Arch. Microbiol. 163, 329–336.

He, Z.B., Maurice, J.-L., Lee, C.S., Gohier, A., Legagneux, P., Pribat, D., Cojocaru, C.S., 2011. Etchant-induced shaping of nanoparticle catalysts during chemical vapour growth of carbon nanofibres. Carbon 49, 435.

Hu, Z., Xia, X., Tang, L., 2004. Process for synthesizing oil and surfactant-free hyaluronic acid nanoparticles and microparticles. US Patent App. 20, 060/040,892.

Ibrahim, S., Ramamurthi, A., 2008. Hyaluronic acid cues for functional endothelialization of vascular constructs. J. Tissue Eng. Regener. Med. 2, 22–32.

Jiang, D., Liang, J., Noble, P.W., 2011. Hyaluronan as an Immune Regulator in Human Diseases. Physiol. Rev. 91, 221–264.

Kakizaki, I., Takagaki, K., Endo, Y., Kudo, D., Ikeya, H., Miyoshi, T., Baggenstoss, B.A., Tlapak-Simmons, V., Kumari, K., Nakane, A., Weigel, P.H., Endo, M., 2002. Inhibition of hyaluronan synthesis in *Streptococcus equi* FM100 by 4-methylumbelliferone. Eur. J. Biochem. 269, 5066–5075.

Kamal, F., Samadi, N., Assadi, M.M., Moazami, N., Fazeli, M.R., 2001. Mutagenesis of Leuconostoc Mesenteroides and selection of Dextransucrase hyperproducing strains. DARU J. Pharm. Sci. 9 (3–4), 18–23.

Laemmli, L.K., 1970. Cleavage of structural proteins during the assembly of the head of bacteriophage T4. Nature 227, 680–685.

Lepidi, S., Grego, F., Vindigni, V., Zavan, B., Tonello, C., Deriu, G.P., Abatangelo, G., Cortivo, R., 2006. Hyaluronan Biodegradable Scaffold for Small-caliber Artery Grafting: Preliminary Results in an Animal Model. Eur. J. Vasc. Endovasc. Surg. 32, 411–417.

Meyer, K., Palmer, J.W., 1943. The polysaccharide of the vitreous humor. J. Biol. Chem. 114, 629–633.

Oh, E.J., Park, K., Kim, K.S., Kim, J., Yang, J.-A., Kong, J.H., Lee, M.Y., Hoffman, A.S., Hahn, S.K., 2010. Target specific and long-acting delivery of protein, peptide, and nucleotide therapeutics using hyaluronic acid derivatives. J. Control. Release 141, 2–12.

Park, H.K., Lee, S.J., Oh, J.S., Lee, S.G., Jeong, Y., Lee, H., 2015. Smart Nanoparticles Based on Hyaluronic Acid for Redox-Responsive and CD44 Receptor-Mediated Targeting of Tumor. Nanoscale Res. Lett. 10, 288.

Prawel, D.A., Dean, H., Forleo, M., Lewis, N., Gangwish, J., Popat, K.C., Dasi, L.P., James, S.P., 2014. Hemocompatibility and Hemodynamics of Novel Hyaluronan-Polyethylene Materials for Flexible Heart Valve Leaflets. Cardiovascular Eng. Technol. 5, 70–81.

Rumora, A.E., Kolodziejczak, K.M., Wagner, A.M., Núñez, M.E., 2008. Thymine Dimer-Induced Structural Changes to the DNA Duplex Examined with Reactive Probes. Biochemistry 47 (49), 13026–13035.

Saranraj, P., Sivakumar, S., Sivasubramanian, J., Geetha, M., 2011. Production, optimization and spectroscopic studies of hyaluronic acid extracted from *Streptococcus pyogenes*. Int. J. Pharm. Biol. Arch. 2 (3), 954–959.

Saravanakumar, G., Choi, K.Y., Yoon, H.Y., Kim, K., Park, J.H., Kwon, I.C., Park, K., 2010. Hydrotropic hyaluronic acid conjugates: Synthesis, characterization, and implications as a carrier of paclitaxel. Int. J. Pharm. 394, 154–161.

Tan, X., Lin, C., Fugetsu, B., 2009. Studies on toxicity of multi-walled carbon nanotubes on suspension rice cells. Carbon 47, 3479–3487.

Thoma, R.W., 1971. Use of mutagens in the improvement of production strains of microorganisms. Folia Microbiologica 16, 197–204.

Torchilin, V.P., 2007. Nanocarriers. Pharm. Res. 24, 2333–2334.

Vázquez, J.A., Pastrana, L., Piñeiro, C., Teixeira, J.A., Pérez-Martín, R.I., Amadom, I.R., 2015. Production of Hyaluronic Acid by *Streptococcus zooepidemicus* on Protein Substrates Obtained from Scyliorhinuscanicula Discards. Mar. Drugs 13, 6537–6549.

Volpi, N., Schiller, J., Stern, R., Soltés, L., 2009. Role, metabolism, chemical modifications and applications of hyaluronan. Curr. Med. Chem. 16, 1718–1745.

Zhu, Y., Crewe, C., Scherer, P.E., 2016. Hyaluronan in adipose tissue: Beyond dermal filler and therapeutic carrier. Sci. Transl. Med. 8, 323ps324.